ICIC Express Letters
Part B: Applications
Volume **8**, Number **7**, July **2017**

ICIC International ©2017 ISSN 2185-2766
pp. **1077–1084**

AN IMPROVED ACCELEROMETER TWELVE-POSITION CALIBRATION METHOD BASED ON REGULAR PARTICLE FILTER

Jihua Zhu, Ling Lv, Yongle Lu, Yan Wang, Yue Yu and Yu Liu

Chongqing Municipal Level Key Laboratory of Photoelectronic Information Sensing
and Transmitting Technology
Chongqing University of Posts and Telecommunications
No. 2, Chongwen Road, Nan'an District, Chongqing 400065, P. R. China
liuy@cqupt.edu.cn; m15938665319@163.com

Received March 2017; accepted May 2017

Abstract. *In the inertial navigation system, an incomplete compensation for MEMS accelerometer bias, scale factor and installation error will affect its accuracy, and then cause roll angle error, pitch angle error in the initial alignment stage. As to the problem, the method that regularized particle filter (RPF) is used to filter the original data of the accelerometer is proposed, which establishes the relationship between the MEMS accelerometer's zero deviation, the scale factor, the installation error and the measured value of the MEMS accelerometer by means of the twelve-position method, and thus gets the mathematical model of accelerometer calibration of twelve-position based on RPF. The experimental results show that the output value of the calibrated MEMS accelerometer is closer to the standard value, and the absolute error of the pitch angle is reduced by 0.70°, which proves the feasibility and validity of the calibration method, and is a good theoretical and practical value in improving the accuracy of the MEMS accelerometer.*
Keywords: MEMS accelerometer, Regular particle filter, Twelve-position, Calibration

1. **Introduction.** In order to improve the accuracy of MEMS inertial navigation system, the relative error of the model established in each of the MEMS inertial sensor, the inertial measurement system must be calibrated before using [1]. Calibration is a key process of using an inertial navigation system. The calibration of the sensor data used by inertial navigation system can eliminate the inertial sensor repeatability error caused by manufacturing defects [2].

Many scholars at home and abroad put forward different accelerometer calibration models; for example, in the work of [3], Chen et al. proposed the method of the test equipment without the directional six-position 24-point. It has little calculation, but it cannot ensure the accuracy of calibration, because it cannot ensure that the X, Y, Z axes in 6-state four sampling points are orthogonal in the actual process. Lu et al. used the method of 6-position calibration of the accelerometer based on the sub-temperature section to establish the error compensation model of the accelerometer, which effectively compensated the temperature drift error caused by the change of the sensor temperature [4]. Prikhodko et al. came up with the way to improve IMU accelerometer rapid calibration model which does not require the use of turntable, but the accuracy is very low [5]. Syed et al. proposed a new method of the multi-position calibration, which does not require special installation and alignment of the inertial sensors, but the process of calculation is too complex to limit the applied range of this method [6,7].

Aiming at the problems that appeared in the calibration model of the accelerometer, an method of the improved accelerometer twelve-position calibration based on the regular particle filter is proposed, which firstly uses the regular particle filter to eliminate the random noise carried by the original data of the accelerometer, and calculates two sets of accelerometer error coefficient by the twelve-position calibration model, then adjusts

error coefficient through the threshold method, and finally we can get a group of accurate calibration coefficients. The principle of the method proposed in this paper is simple, the calculation is small, in the absence of turntable it can also be completed, so it has a wide range of applications. The experimental results show that the method proposed in this paper is more accurate.

2. **The Theory of Regularized Particle Filter (RPF).** In the resampling phase, conventional particle filtering uses the discreted particles, and the sampling process causes the particles to lose diversity, resulting in sample depletion. At the beginning of the twentieth century, Musso proposed regularized particle filter (RPF) to solve the above problem.

A nonlinear discrete-space state model can be represented by the state equation and the observed equation as Equation (1) and Equation (2) [8].

$$x_k = f(x_{k-1}, w_{k-1}) \tag{1}$$

$$z_k = h(x, v_k) \tag{2}$$

where x_k, z_k are the k time system state vector and k time system observation vector, w_k is the system noise, v_k is the observation noise, and they are independent of each other. $f(\cdot)$ and $h(\cdot)$ are two known non-linear mapping functions.

If $\{x_{0:k}^i, w_k^i\}_{i=1}^N$ is a random particle, $p(x_{0:k}|z_{1:k})$ is the posterior probability density function, $\{x_{0:k}^i, i = 0, 1, \ldots, N\}$ is the corresponding set of particles, it contains all states from 0 to k.

Regularized particle filtering improved the particle filtering during the resampling process, that is sampling from the continuous approximation density of the posterior density. If [9,10]:

$$\left\{x_k^i, w_k^i\right\}_{i=1}^N \sim p(x_k|z_{1:k}) \approx \sum_{i=1}^N w_k^i K_s\left(x_k - x_k^i\right) \tag{3}$$

where $K_s(x) = \frac{1}{s^{n_x}} K(\frac{x}{s})$ is the scale that can be adjusted Kernel density, s is the core of the bandwidth, which is greater than zero, n_x described the state of the dimension, and w_k^i is the normalized coefficient.

The posterior probability distribution at k time can be approximated after normalization, and the RPF algorithm implementation process can be approximated as shown in Table 1. Regularized particle filter compared with the traditional particle filter, increased the nuclear density of the process, so they have the similar complexity.

TABLE 1. RPF algorithm flow

(1) $i = 1 : N$
extract $x_k^i \sim p(x_k|x_{k-1}^i)$, calculate the weights $w_k^i = p(z_k|x_k^i)$
(2) normalized weight: $\hat{w}_k^i = \frac{w_k^i}{\sum_{i=1}^N w_k^i}$
(3) calculate the number of effective particles: $N_{eff} = \frac{1}{\sum_{i=1}^N (w_k^i)^2}$
(4) if $N_{eff} < N_{thr}$
calculate the empirical matrix S_k, and make $D_k D_k^T = S_k$
(5) re-sampling: $\left[\left\{x_k^j, w_k^j\right\}_{j=1}^N\right] = resample\left[\left\{x_k^i, w_k^i\right\}_{i=1}^N\right]$
(6) $i = 1 : N$
use the Epanechnikov/Gauss to extract $\varepsilon^i \sim K$, let $x_k^{i^*} = x_k^i + h_{opt} D_k \varepsilon^i$

3. Improved Twelve-Position Calibration Model of MEMS Accelerometer.

3.1. **The principle of the six-position method.** The error factors of MEMS accelerometers are mainly zero bias, scale factor, installation error, etc. We get the error model of MEMS accelerometer based on these error factors.

$$\begin{bmatrix} A_x - a_{x0} \\ A_y - a_{y0} \\ A_z - a_{z0} \end{bmatrix} = \begin{bmatrix} k_x & k_{xy} & k_{xz} \\ k_{yx} & k_y & k_{yz} \\ k_{zx} & k_{zy} & k_z \end{bmatrix} \cdot \begin{bmatrix} a_x \\ a_y \\ a_z \end{bmatrix} \tag{4}$$

where A_x, A_y, A_z are the actual measured values of the MEMS accelerometer; a_{i0} $(i = x, y, z)$ is the zero bias of the three-axis of the MEMS accelerometer; k_i $(i = x, y, z)$ is the non-orthogonal error between the three axes of the MEMS accelerometer.

3.2. **Twelve-position calibration scheme of MEMS accelerometer.** This paper presents a twelve-position static flip-up experiment calibrated MEMS accelerometer. The twelve-position orientation of the MEMS accelerometer and the gravitational acceleration values for each axis are shown in Table 2.

Table 2. The twelve-position orientation of the MEMS accelerometer and the gravitational acceleration value of each axis

position	coordinate axis			gravity acceleration value/g		
	Z	Y	X	Z	Y	X
1	upward	east	south	−1	0	0
2	south	east	down	0	0	1
3	north	east	north	1	0	0
4	north	east	upward	0	0	−1
5	south	upward	east	0	−1	0
6	down	south	east	1	0	0
7	north	down	east	0	1	0
8	upward	north	east	−1	0	0
9	east	south	upward	0	0	−1
10	east	down	south	0	1	0
11	east	north	down	0	0	1
12	east	upward	north	0	−1	0

The design of MEMS accelerometer calibration scheme is as follows:

(1) Fix MEMS-IMU in the center of the dual-axis electric turntable, MEMS accelerometer Z axis perpendicular to the turntable table, and X, Y axis parallel to the turntable table;

(2) The IMU is preheated for 10 minutes. When the IMU enters a steady state, the turntable is manipulated so that the Z axis is rotated by 0°, 90°, 180°, 270°, and the IMU output data is collected during rotation. The sampling frequency is 50Hz, and we collect 40 seconds of data on each sample point;

(3) Adjust the turntable position, control the turntable, making the Y, X axis at 0°, 90°, 180°, 270°, and collect the four locations of the MEMS accelerometer output voltage value;

(4) Organize the collected MEMS accelerometer output voltage value, and calculate the scale factor, zero position and installation error of the MEMS accelerometer according to the output voltage value of the accelerometer output value of twelve-position points;

(5) Bring the zero bias, scale factor, installation error and other parameters into the MEMS accelerometer error model, and calibrate accelerometer.

3.3. **Determination of error parameters of MEMS accelerometer.** According to the MEMS model described in Section 3.1, we regard the output of the accelerometer voltage as the input of the error model, which are the voltage of X, Y and Z axis at the position of 90° and 270° (the positions are 1, 3, 5, 7, 9 and 11), and we can get the first group of MEMS accelerometer error parameters. According to the output of the MEMS accelerometer, we can get a group of error model coefficients.

$$\begin{cases} a_{x0_1} = \frac{A_{x1_1}+A_{x2_1}+A_{x3_1}+A_{x4_1}+A_{x5_1}+A_{x6_1}}{6} \\ k_{xz_1} = \frac{A_{x2_1}-A_{x1_1}}{2},\ k_{xy_1} = \frac{A_{x4_1}-A_{x3_1}}{2},\ k_{x_1} = \frac{A_{x6_1}-A_{x5_1}}{2} \end{cases} \tag{5}$$

$$\begin{cases} a_{y0_1} = \frac{A_{y1_1}+A_{y2_1}+A_{y3_1}+A_{y4_1}+A_{y5_1}+A_{y6_1}}{6} \\ k_{yz_1} = \frac{A_{y2_1}-A_{y1_1}}{2},\ k_{y_1} = \frac{A_{y4_1}-A_{y3_1}}{2},\ k_{yx_1} = \frac{A_{y6_1}-A_{y5_1}}{2} \end{cases} \tag{6}$$

$$\begin{cases} a_{z0_1} = \frac{A_{z1_1}+A_{z2_1}+A_{z3_1}+A_{z4_1}+A_{z5_1}+A_{z6_1}}{6} \\ k_{z_1} = \frac{A_{z2_1}-A_{z1_1}}{2},\ k_{zy_1} = \frac{A_{z4_1}-A_{z3_1}}{2},\ k_{zx_1} = \frac{A_{z6_1}-A_{z5_1}}{2} \end{cases} \tag{7}$$

Similarly, we regard the output of the accelerometer voltage as the input of the error model, which are the voltages of X, Y and Z axis, respectively, at the position of 90° and 270° (the positions are 2, 4, 6, 8, 10 and 12 in Table 2), and we can get the second set of MEMS accelerometer error parameters.

The error model parameters of the three groups of MEMS accelerometers are processed by the threshold method, and the simplified model parameters are obtained as follows:

$$a_{x0} = \alpha a_{x0_1} + \beta a_{x0_2},\ k_x = \alpha k_{x_1} + \beta k_{x_2},\ k_{xz} = \alpha k_{xz_1} + \beta k_{xz_2},\ k_{xy} = \alpha k_{xy_1} + \beta k_{xy_2} \tag{8}$$

$$a_{y0} = \alpha a_{y0_1} + \beta a_{y0_2},\ k_{yz} = \alpha k_{yz_1} + \beta k_{yz_2},\ k_y = \alpha k_{y_1} + \beta k_{y_2},\ k_{yx} = \alpha k_{yx_1} + \beta k_{yx_2} \tag{9}$$

$$a_{z0} = \alpha a_{z0_1} + \beta a_{z0_2},\ k_{zx} = \alpha k_{zx_1} + \beta k_{zx_2},\ k_z = \alpha k_{z_1} + \beta k_{z_2},\ k_{zy} = \alpha k_{zy_1} + \beta k_{zy_2} \tag{10}$$

In Equation (8), Equation (9) and Equation (10), the weighting coefficients are given: $\alpha = \beta = 0.5$.

4. Experimental Verification.

4.1. **Experimental apparatus.** (1) MEMS-IMU. MEMS-IMU developed for the laboratory is based on the attitude of the MEMS sensor that integrates a 3-axis accelerometer, a 3-axis gyroscope, a 3-axis magnetometer, and a barometer, which is shown in Figure 1.

FIGURE 1. Self-made attitude instrument

(2) Double-axis electric turntable. 902E-1 biaxial electric turntable is produced by Beijing Institute of Aeronautical Precision Machinery, which can provide input angular velocity for the attitude meter, and turntable speed accuracy is 1×10^{-3} ($\pm 0.01(^\circ)/\text{s} \sim \pm 100(^\circ)/\text{s}$), as shown in Figure 2.

The output of the MEMS accelerometer is affected by random noise, and the data is very unstable. In order to ensure the accuracy of the error model, the output value of the MEMS accelerometer is processed by RPF filtering before the calibration coefficient is calculated. In this paper, the output value of the MEMS accelerometer is filtered, and

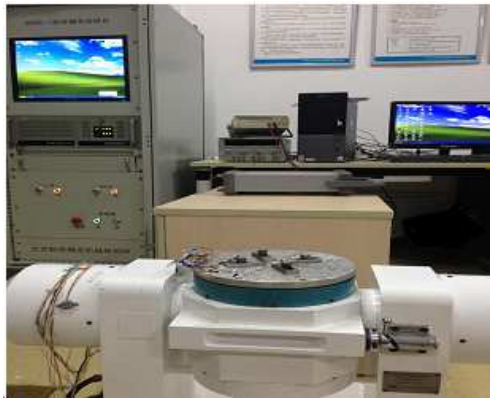

FIGURE 2. 902E-1 double-axis electric turntable

the contrast is shown in Figure 3. It can be observed from Figure 3 that RPF filtering is a good way to eliminate the random noise of the MEMS accelerometer, which ensures the effectiveness of the MEMS accelerometer output value.

The data of the MEMS accelerometer X-axis, Y-axis and Z-axis are brought into the Equation (8) to Equation (10), can get the error parameters of MEMS accelerometer. The sensitivity Z axis of the MEMS accelerometer is placed vertically on the biaxial electric turntable. A number of data are collected into the error model of the MEMS accelerometer. The comparison of the calibrated value before and after the MEMS accelerometer is shown in Figure 4. The sensitivity axis of the MEMS accelerometer is placed vertically on the biaxial electric turntable. The output value of the MEMS accelerometer before and after calibration is shown in Table 3. Table 3 shows that the calibrated accelerometer output value is closer to the standard value, and the effect is more obvious.

TABLE 3. Calibrate the output value before and after calibration

sensitive axis	the accelerometer output value before the calibration/(m/s^2)	the accelerometer output value after the calibration/(m/s^2)
X	0.1764706	0.008706
Y	0.7794118	0.024124
Z	9.647058	9.788650

The MEMS accelerometer output value solves the pitch angle and roll angle of the MEMS-IMU attitude meter, so it can be used to verify the calibration effect of the MEMS accelerometer. Taking the pitch angle as an example, the pitch angle of the MEMS-IMU attitude instrument is $-60°, \ldots, 60°$ on the turntable in the range of $-90° \sim 90°$. The pitch angle of the attitude meter is calculated by the data before and after calibration with the MEMS accelerometer. The results are shown in Table 4.

It can be seen from Table 4, MEMS accelerometer calibration output value after the settlement of the pitch angle and the actual input value of the turntable is closer, in the pitch angle of $-90° \sim 90°$ range, the average absolute error of the pitch angle after calibration is 0.28°, and the average value of the absolute error of the pre-calibration pitch angle is 0.98°, which verifies the feasibility and effectiveness of the modified accelerometer twelve-position calibration method based on the regular particle filter.

Use the algorithm proposed in this paper, the algorithms proposed in [4] and [7], to respectively calibrate the accelerometer. Then taking advantage of the calibrated accelerometer data to calculate the roll angle of the IMU, the root-mean-square error (RMSE) is shown in Table 5. According to the comparison of the three sets of data, the algorithm of calibration accelerometer proposed in this paper has a better result.

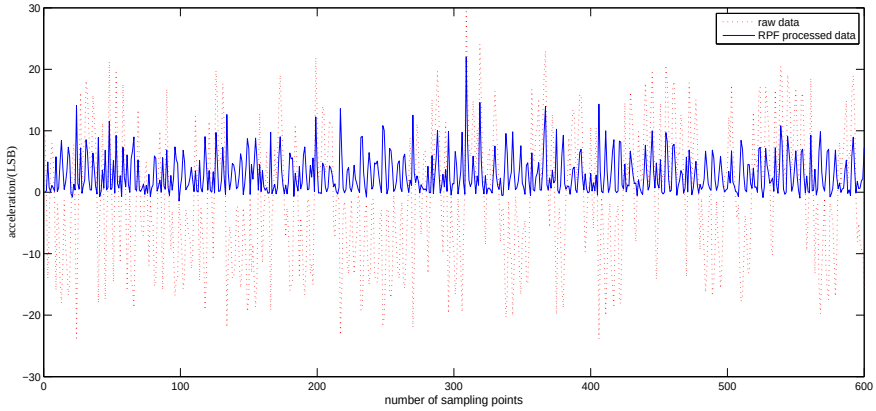

(a) Accelerometer X axis data

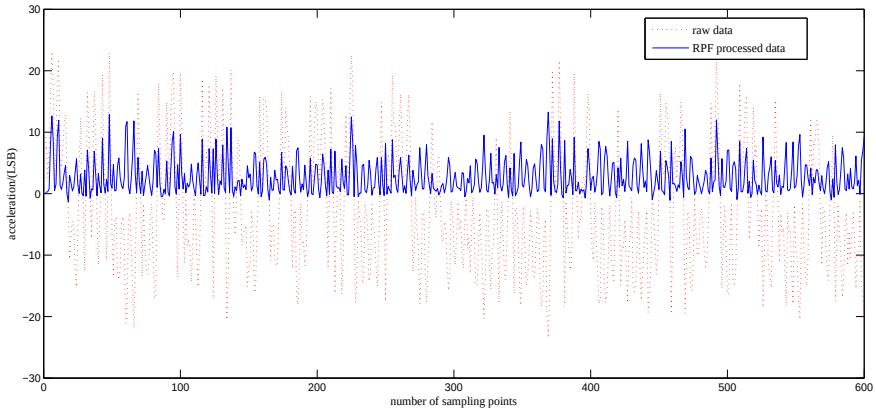

(b) Accelerometer Y axis data

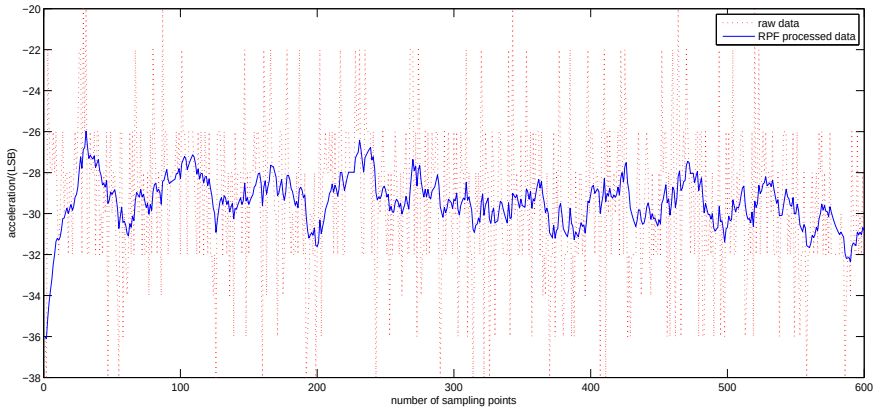

(c) Accelerometer Z axis data

FIGURE 3. The comparison chart before and after the RPF filter

5. **Conclusions.** The innovation of the paper is firstly to eliminate the random noise carried by the original data of the accelerometer by using the regular particle filter, and calculate the error coefficient of the two accelerometers by the twelve-position calibration model, and then adjust the error coefficient by the threshold method, and finally get the accurate accelerometer calibration coefficient. The experimental data analysis shows that the calibrated MEMS accelerometer output value is closer to the standard value, in the range of $-90° \sim 90°$, the pitch error is reduced by 0.70°. The principle of this method

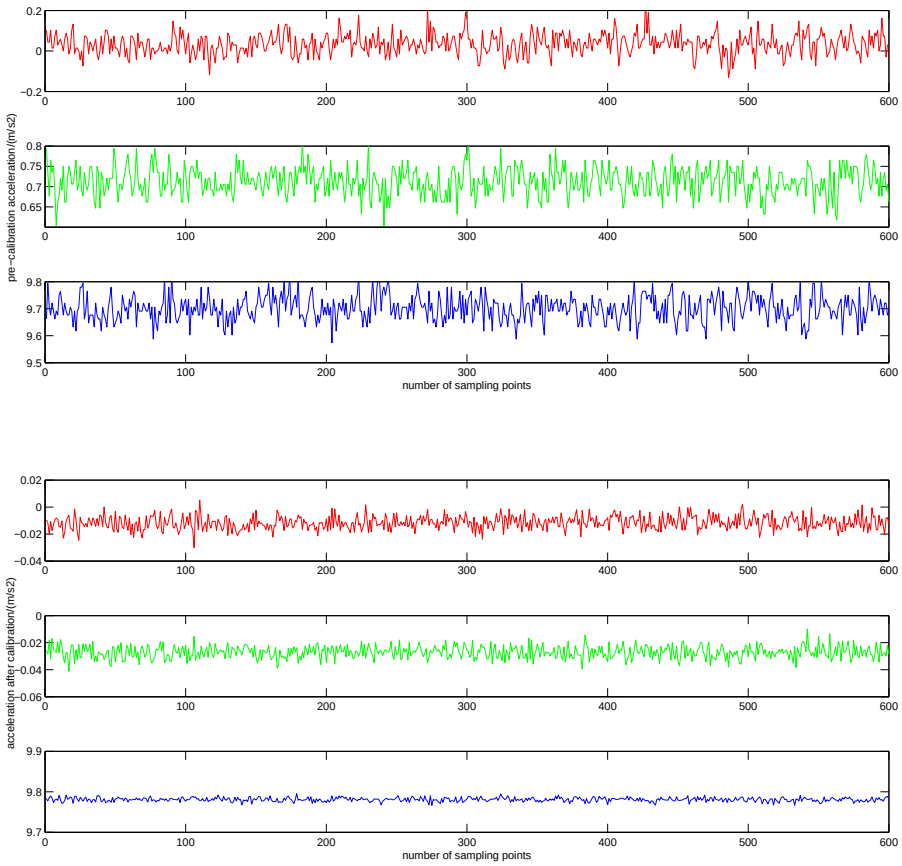

FIGURE 4. Comparison of MEMS accelerometer before and after calibration

TABLE 4. The pitch angle error before and after calibration

turntable input/(°)	pre-calibration output/(°)	output after calibration/(°)	absolute error before calibration/(°)	absolute error after calibration/(°)
−60	−58.39	−59.65	1.61	0.35
−50	−48.89	−49.69	1.11	0.31
−40	−38.94	−40.32	1.06	0.32
−30	−28.96	−29.84	1.04	0.16
−20	−19.85	−20.10	0.15	0.10
−10	−9.89	−9.86	0.11	0.14
0	0.38	0.43	0.38	0.43
10	10.18	10.15	0.18	0.15
20	20.30	20.50	0.30	0.50
30	28.95	29.76	1.05	0.24
40	38.70	39.67	1.3	0.33
50	48.69	49.82	1.31	0.18
60	58.54	59.67	1.46	0.33

TABLE 5. The root mean square error of roll angle and pitch angle

algorithm	roll angle (°)	pitch angle (°)
The algorithm proposed in [4]	1.35	1.40
The algorithm proposed in [7]	1.05	0.93
The algorithm proposed in this paper	0.75	0.42

which has a good theoretical and engineering value to improve the accuracy of MEMS accelerometer measurement, is simple and easy to implement with high precision.

Acknowledgment. This work is funded in part by the International Joint Research Center Technology Platform and Base Construction (cstc2014gjhz0038), the Doctoral Scientific Research Foundation of Chongqing Univ. of Posts and Telecommunications (A2015-40, A2016-72, A2016-76), Chongqing Research Program of Foundation and Advanced (cstc2015jcyjBX0068), Chongqing Key Laboratory of Photoelectronic Information Sensing and Transmitting Technology (cstc2014pt-sy40001), the National Natural Science Foundation of Chongqing Univ. of Posts and Telecommunications (A2015-49), University Innovation Team Construction Plan Funding Project of Chongqing (Architecture and core technologies of smart medical system) (CXTDG201602009). We also gratefully acknowledge the helpful comments and suggestions of the reviewers, which have improved the presentation.

REFERENCES

[1] S. Wang, Current status and applications of MEMS sensors, *MEMS and Sensors*, vol.48, no.8, pp.516-522, 2011.

[2] L. M. C. Brasca, P. Bernardi and M. S. Reorda, A parallel tester architecture for accelerometer and gyroscope MEMS calibration and test, *Journal of Electronic Testing*, vol.27, no.3, pp.389-402, 2011.

[3] B. Chen, W. Sun and G. Zhang, Strapdown unit (without orientation) six-position test calibration, *Missile and Space Vehicle*, vol.3, no.3, pp.23-27, 2001.

[4] C. Lu, R. Li, J. Liu and Y. Hang, Combined error modeling for 3D-MEMS accelerometer in MIMU, *Journal of Test and Measurement Technology*, vol.25, no.1, pp.29-34, 2011.

[5] I. P. Prikhodko, C. Merritt and J. A. Gregory, Continuous self-calibration canceling drive-induced errors in MEMS vibratory gyroscopes, *The 18th International Conference on Solid-State Sensors, Actuators and Microsystems (TRANSDUCERS)*, pp.35-38, 2015.

[6] Z. F. Syed, P. Aggarwal and C. Goodall, A new multi-position calibration method for MEMS inertial navigation systems, *Measurement Science and Technology*, vol.18, no.7, p.1897, 2007.

[7] J. O. Nilsson, I. Skog and P. Händel, Aligning the forces – Eliminating the misalignments in IMU arrays, *IEEE Trans. Instrumentation and Measurement*, vol.63, no.10, pp.2498-2500, 2014.

[8] T. Willemsen, F. Keller and H. Sternberg, Concept for building a MEMS based indoor localization system, *2014 International Conference on Indoor Positioning and Indoor Navigation (IPIN)*, pp.1-10, 2014.

[9] N. Merlinge, K. Dahia and H. Piet-Lahanier, A box regularized particle filter for terrain navigation with highly non-linear measurements, *IFAC-PapersOnLine*, vol.49, no.17, pp.361-366, 2016.

[10] A. Gonczarek and J. M. Tomczak, Articulated tracking with manifold regularized particle filter, *Machine Vision and Applications*, vol.27, no.2, pp.275-286, 2016.